

# Evaluation of Creep and Shrinkage of Lightweight Concrete Beams containing Tuff Aggregates

Ezekiel Mariita\*, Siphilia Mumenya\*\*, John Mwero\*\*\*

\* Postgraduate Student; Department of Civil & Construction Engineering, University of Nairobi, 30197-00100, Nairobi, Kenya.

\*\* Associate Professor, Department of Civil & Construction Engineering, University of Nairobi, 30197-00100, Nairobi, Kenya.

\*\*\* Associate Professor, School of Civil and Resource Engineering, Technical University of Kenya, 52428-00200, Nairobi, Kenya.

\*\* Department, Institute Name, if any

DOI: 10.29322/IJSRP.13.09.2023.p14124

<https://dx.doi.org/10.29322/IJSRP.13.09.2023.p14124>

Paper Received Date: 15th August 2023

Paper Acceptance Date: 15th September 2023

Paper Publication Date: 26th September 2023

## Abstract

The aim of the study was to evaluate creep and shrinkage of concrete beams containing tuff aggregates (TA) as a partial replacement of coarse aggregate (CA). This was done at 0, 12.5, 25, 50, 75 and 100 % replacement levels. The methods used was characterization of TA, CA and Fine Aggregates (FA), mineralogical characterization of TA, compressive strength, modulus of elasticity of the cast concrete and loading 0.2 x 0.2 x 1.0 m beam specimens with dead weights for 60 days. Four beams of C45 were cast to test creep, whereby two had 0 % replacement and another two had 100 % replacement levels of CA. In each of the two sets, one beam was testing for creep deformation while another unsealed was tested for shrinkage. The maximum value of 0.00317 mm/m and 0.000236 mm/m of the 0 % and 100 % replacements were measured. However, there was an increase in shrinkage with time. Shear strain increased with time, whereby Normal Weight Concrete (NWC) produced lower values than Light Weight Concrete (LWC). The strain of reinforcements for the NWC and LWC was measured to be 0.000473 mm/m and 0.000427 mm/m, respectively. LWC experienced higher total bottom strains (creep + shrinkage included) than NWC at 694 and 360 micro strains, respectively. LWC produced higher creep coefficient values of 1.63 while NWC was 0.6. ACI and BS EN models produced a value of 0.64 and 0.597, respectively. Thus, it is concluded that LWC produces lower compressive strength, modulus of elasticity, and higher creep values than NWC. NWC experiences higher shrinkage than LWC owing to continued internal curing that reduces autogenous shrinkage.

## Index Terms

Creep; shrinkage; tuff aggregates; lightweight concrete;

## I. INTRODUCTION

Tuff refers to various deposits from volcanic eruptions containing high-silica magmas [1]. It is classified as a lightweight aggregate and used to produce lightweight concrete. Some advantages of volcanic tuff include its high surface area, highly porous structure, and low density. It is available in different types, sizes, and colours and can reduce concrete dead weight [2], [3]; Various studies have examined the use of volcanic tuff as a light weight aggregate, building stone, or as a pozzolan for cement and concrete production [1]; [3];[4];[5];[6].



Figure 1: Tuff Aggregates heap [6]

Creep refers to the strain or deformation of a solid material due to long-term sustained load/stress. It is a phenomenon that causes the deformation of concrete to increase with time under sustained loading, as shown in Figure 2 [7]. Creep originates and develops in the Calcium Silicate hydrates (C-H-S) of hardened Portland cement paste [8]; [9].

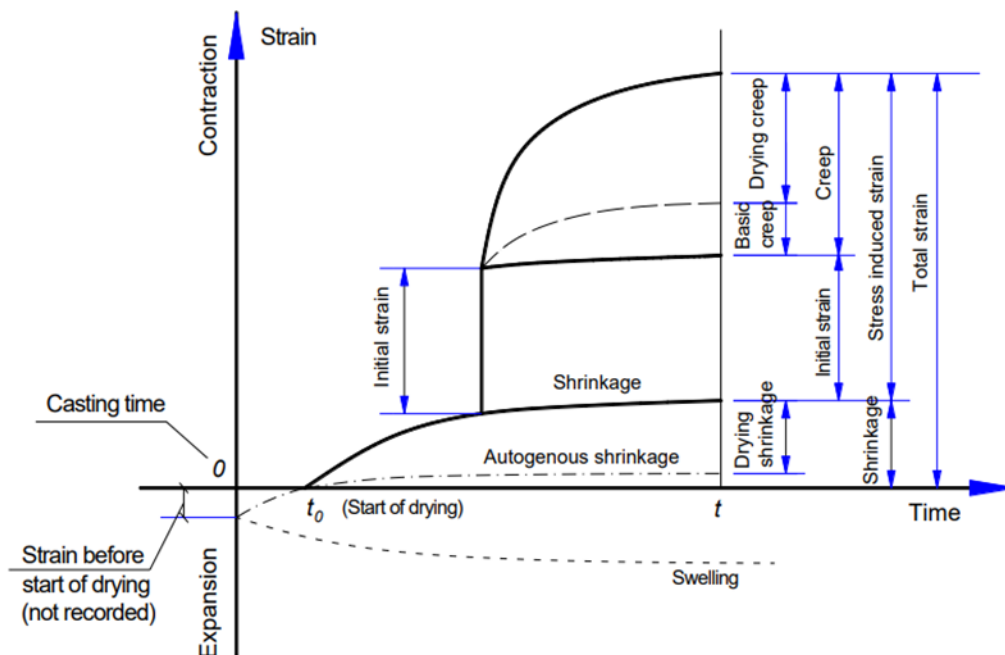


Figure 2: Development of the Creep-Strain under sustained load [7]

Several internationally recognized models are used to predict creep strain without laboratory test setups. They include the BS 1881 (1985) method, BS EN 1992-1-1: 2004, B3 (Bazant-Baweja), ACI 209R-92, GL2000 (Gardner and Lockman), CEB MC90-99, and the AS3600-2009 (Australian standard; [10];[11]; ACI Committee 209.R-08, 2008; [9]. According to Brooks (2015), the four most current models are BS EN 1992-1-1: 2004, ACI 209R-92, B3 (Bazant-Baweja), and GL2000 (Gardner and Lockman). These models are based on experience, observation, and logic and thus vary widely in their application and have various intrinsic and extrinsic variables, as shown in Table 1[15]. Despite the development of these models, some researchers have noted their inaccuracy and unreliability [13];[14].

Table 1. Models of predicting Creep and the various factors accounted for in each Model[15]

Factors Accounted by Different Prediction Methods		Various Creep Prediction Models						
		ACI 209 (1992)	AS 3600 (1998)	BS 8110 (1985)	CEB-FIP (1978)	CEB-FIP (1990)	SABS 0100 (1992)	RILEM B3 (1995)
Intrinsic factors	Aggregate type						✓	
	Aggregate/Cement Ratio							✓
	Air content							
	Cement Content				✓	✓		
	Cement type					✓		✓
	Concrete density		✓					
	Fine total aggregate ratio	✓						
	Water to Cement ratio	✓				✓		✓
	Water content							✓
	Extrinsic Factors	Age at 1 <sup>st</sup> Instance of Loading	✓	✓	✓	✓	✓	✓
Age of sample								✓
Stress from an applied load		✓	✓	✓	✓	✓	✓	✓
f <sub>cu</sub> of Concrete at Loading							✓	
Cross-sectional shape								✓
Time of Loading		✓	✓		✓	✓		✓
Effective thickness		✓	✓	✓	✓	✓	✓	✓
E <sub>c</sub> at the age of loading				✓			✓	✓
Relative humidity		✓	✓	✓	✓	✓	✓	✓
Temperature						✓		✓
Time drying begins								✓

Saradhi Babu [21] summarized the relationship of the Modulus of Elasticity to the particle density by various researchers and code provisions for LWA. It can be observed that within the same particle density, the average variation of the minimum to the maximum modulus of elasticity can be 3- 9 GPa. However, it can be noted from the study of Chen et al. (2003), Particle density of 1.5 g/cm<sup>3</sup> produces 25 GPa. In this study, the particle density was 1.885 g/cm<sup>3</sup>, which is not in the range presented in Figure 3. In this study, the values of particle density are used in the computation of specific creep using Counto Model.

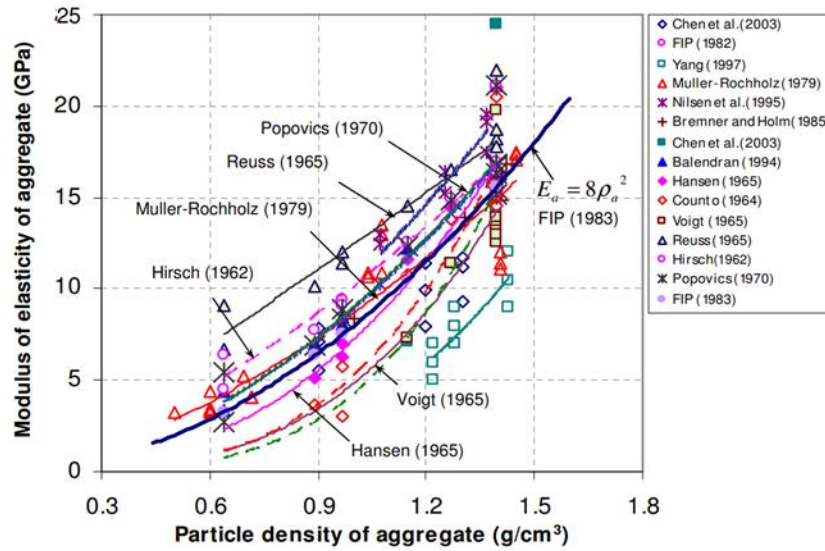


Figure 3: A graph of particle density against Modulus of Elasticity of Aggregates [21].

### Specific Creep of Concrete from Counto Model

Brooks [11] noted that there are parallel and series models to evaluate the elastic modulus of concrete by a two-phase model subjected to external loading, temperature, and humidity. These models correspond to strain compatibilities and equilibrium of forces. The phases have different properties for stress-strain behaviour, temperature, and time-dependent movements. Chiorino [26] proposed a mathematical specific creep model that takes account of a fractional volume of aggregates in the concrete, w/c, Modulus of Elasticity of Matrix Phase, specific creep of the cement paste matrix, relative humidity, volume/surface, time effects, compressive strength of the cement paste, and the applied stress to the structural element.

The Counto's Specific Creep Model is;

$$C_c(t, t_o) = (1 - g^{0.5}) \times \left[ \frac{1}{E'_m(t, t_o)} - \frac{1}{E_m t_o} \right] + \frac{\left( \frac{1-g^{0.5}}{g^{0.5}} \right) \cdot (E_m(t_o) - E'_m(t, t_o))}{\left[ E_a + \left( \frac{1-g^{0.5}}{g^{0.5}} \right) \times E'_m(t, t_o) \right] \left[ E_a + \left( \frac{1-g^{0.5}}{g^{0.5}} \right) \times E_m(t_o) \right]} \quad (1)$$

Where;

$E_a$  is the Modulus of Elasticity of aggregate matrix (whereby NA is 60000 Mpa & TA is 25000 Mpa).

The  $E'_m(t, t_o)$  is the modulus of elasticity (effective) of mortar at age t after loading at the time ( $t_o$ ), where; g is the aggregate volume fraction. For 0 % replacement of TA is 0.6193 and 100 % replacement of TA is 0.6206, and w/c is 0.38.

The specific creep of mortar can be determined using Equation 5 after accounting for relative humidity, time effects and intervals, and v/s area.

$$C_m = \frac{R_{C\infty} \cdot R_{RHt} \times \frac{10000}{f_m^{1.06}}}{22R_a c_{\infty} + t} \quad (3)$$

The values for the modulus of elasticity of cement paste can also be determined by method proposed by Wittmann and Zhao [27], which is derived from the modulus of elasticity of NWA and LWA. The values of the modulus of elasticity of TA can be estimated from the summary of the finding of other researchers, as shown below and adopted from Gaudagnuolo et al [28]. In this study, the Counto Model is used since it contains the various variables that affect creep in LWA.

### 1.1 Objectives

The main objective of the study was to evaluate creep and shrinkage of lightweight concrete containing tuff aggregates.

## II. MATERIALS AND METHODS

### 2.1 CHEMICAL CHARACTERIZATION

This publication is licensed under Creative Commons Attribution CC BY.

<https://dx.doi.org/10.29322/IJSRP.13.09.2023.p14124>

[www.ijsrp.org](http://www.ijsrp.org)

The composition of the lightweight volcanic tuff aggregate used in the study was tested using scanning electron microscopy (SEM) in the Materials Testing and Research Division at the Ministry of Infrastructure and Public Works.

## 2.2 CONCRETE MIX DESIGN

KU Mix Design sheet developed by The University of Kansas was used to optimize the gradation of the tuff aggregates used in concrete where necessary. The concrete mix design process for both tuff and normal-weight concrete was carried out according to ACI 211.2 with a 28th-day design strength of 25, 30, 35, 40, and 45 N/mm<sup>2</sup>, which are the semi-high performance recommended concrete strength class for reinforced structural load-bearing elements [16]. Batching was carried out by the weight of constituent materials to give a unit volume of concrete. The samples were mixed using a mechanical mixer with controlled mixing time and speed. The required conventional coarse aggregate proportions were replaced by weights of 0, 12.5, 25, 50, 75, and 100 % of the tuff aggregate, as shown in Table 2.

In this study, a w/c ratio of 0.38 was used to cast C45 class of concrete that pre-prepared 150 x 150 x 1000 mm beam specimens loaded for testing of creep.

Table 2. Mixture Proportioning of the classes 25,30, 35, 40 and 45 classes of concrete.

Material(s)	Proportion per Cubic. m				
Class of Concrete	C25	C30	C35	C40	C45
Cement	354.10	400.00	459.57	514.29	568.42
Coarse Aggregate	1028.39	1028.39	1028.39	1028.39	1028.39
Fine Aggregate	645.69	645.69	645.69	645.69	645.69
Water	216.00	216	216	216	216
Determined % of Replacement	10.4 %	11.77 %	13.54 %	15.89 %	16.73 %

## 2.3 PLASTIC AND HARDENED CONCRETE TESTS

For plastic concrete tests, the slump was undertaken, while the compressive strength test and modulus of elasticity test were undertaken for hardened tests.

Concrete cubes (150x150x150mm) were prepared, cured at room temperature, and crushed as per BS EN 12390- 2002. The compressive testing ages were on the 28th and 56th day. An average of 3 cubes were tested at each test age according to BS 1881: Part 116.

The modulus of elasticity for the LWC containing tuff aggregates was determined as per BS EN 1992-1-1: 2004 and GB/T 50081-2019.

Two Concrete cubes (150 x 150 x 300 mm) were prepared and cured at room temperature to measure modulus of elasticity. One cube was crushed to failure load, and one-third of the load was used as control load to measure transverse strain using dial gauges.



Figure 4. Modulus of Elasticity Testing Equipment undertaken at the Kenya Expressway Project, Nairobi.

The deformation of the specimen was measured using a Linear Variable Displacement Transducer (LVDT), where two of them are attached with a pair of clamps at a gauge length of 100 mm, as shown in Figure 4. The process for measurement of modulus of elasticity was repeated for two more sets of 2 cubes and average values of the three sets was used as modulus of elasticity values. The results were recorded per the procedures outlined in the Eurocode Standards.

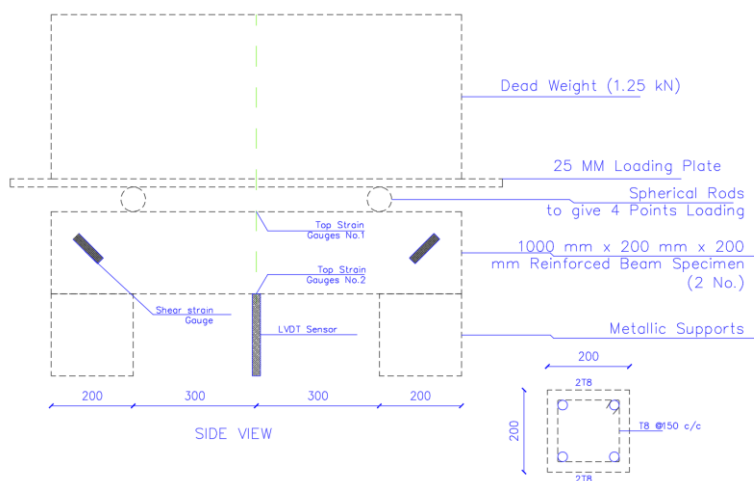
#### 2.4 CREEP TESTING

The Standard Test Method for concrete creep in compression, as stated in ASTM C 512:871, was followed to determine the creep behaviour of both the NWC & LWC containing tuff aggregates. Unsealed specimens were used to determine and evaluate the strain due to creep and shrinkage.

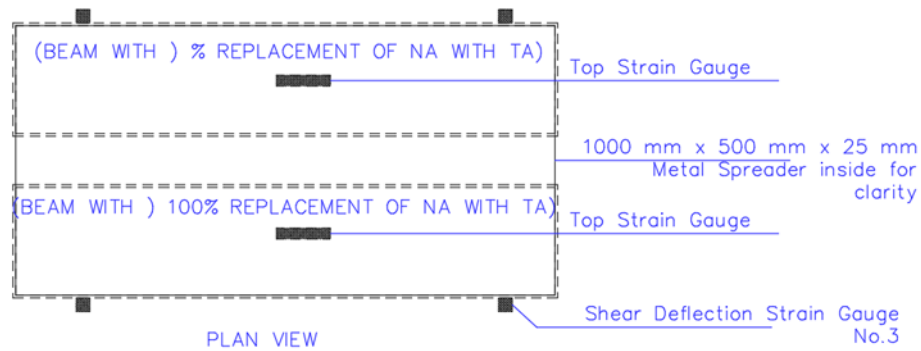
The specimens were bonded in water for 28 days to inhibit capillary depression effects by saturation of the pores. The specimens were placed in environments free of moisture exchange with the surrounding environment. The specimens were later attached with extensometers for strain measurements. They were stored at room temperatures (of 20 OC & a relative humidity of 50-70 %) until the creep tests at 56 days.

Shrinkage strain gauges were placed on the top surface of the flexural region of unsealed beam specimens. They were unsealed to be affected by the variations in temperature and humidity. The temperature range observed for the experiment was 15 to 28°C for March-April 2022, and the average humidity of 70 % in the Juja Area. Strain in the reinforcements were measured using strain gauges attached at middle of the reinforcements.

The author reviewed the various setups for compressive and bending creep testing and this aided in developing a setup using dead weights to measure creep in this study as shown in Figure 5.



(a)



(b)



(c)



(d)

Figure 5. Testing Set-up for bending creep and fabrication proposed by the Author and position of attachment of strain gauges and LVDT Sensors. (a) showing the Side View and (b) Plan View, (c) attachment of strain gauges to the beam specimen and (d) setup showing the beam specimen loaded with dead weights and printout of the strains and displacement by Orion Data Logger.

To ensure constant loading- dead weights were attached to the creep testing specimens to give equivalent stress of 40 % of the ultimate bending strength of the 200 mm x 200 mm reinforced beam specimen. An LVDT sensor connected to Orion Data Logging Systems measured miniature deformations. It displayed the results on a computer screen while a measurement of stresses was done using PFL-30-11-3LJC-F (30 mm long strain gauge for concrete strain) and FLAB-10-11-3LJC-F (10 mm long strain gauges for steel strain). They were ideal for high-strain measurements for the creep test set-up.

### III. RESULTS AND DISCUSSION

#### 3.1 CHEMICAL CHARACTERIZATION

Table 3. Chemical Composition of Tuff Aggregates (%)

Element Name	Used by the Author	[17]	[18]	[19]
		Ababneh & Matalkah, 2018)	Edris et al, 2021)	Maaitah et al, 2015)
Al <sub>2</sub> O <sub>3</sub>	14.471	4.77	4.59	15.2
SiO <sub>2</sub>	71.100	20.8	34.39	50.6
K <sub>2</sub> O	6.580	0.40	1.3	
CaO	1.366	64.6	24.11	9.0
Fe	5.531	3.79	31.46	11.2
MgO		2.52	0.49	5.8

$Na_2O$	0.02
$MnO$	2.5
$P_2O_5$	4.6

Tuff can be classified as Welded Tuff, Rhyolitic Tuff, Trachyte Tuff, Andesitic Tuff, Basaltic Tuff, and Ultramafic Tuff. The Tuff aggregate used in the study is described as trachyte due to minor amounts of mafic minerals as shown in Figure 6 (a) and (b). It is noted that there is 5.531 % of Iron in the mineralogical/chemical composition as shown in chemical composition of TA in Table 3.



Figure 6 (a) Picture of the Tuff Aggregate sample collected from Nakuru in Bahati Area (0.1671° S, 36.1287° E). (b) Close-up View of the Tuff Aggregate described as Trachyte.

Tuff Aggregates have a felsic chemical composition formed from igneous rocks with elements forming quartz and feldspar. Quartz is a crystalline mineral containing silicon dioxide whereby the atoms are joined into a continuous chain of SiO<sub>4</sub> with an atom of oxygen shared between two tetrahedra. The overall chemical compound of quartz is SiO<sub>2</sub>. In this study, the TA used contains 71.10 % of Quartz greater than 69 %, thus described as felsic, making the TA granite-like. This explains the relatively higher SG for this TA when it is compared to those of other researchers. The SG of quartz is 2.65.

Feldspar contains aluminium tectosilicate minerals and either barium, calcium, potassium, or sodium cations. In this study, the TA can be described as either plagioclase or alkali feldspars. Alkali feldspar is the predominant feldspar as the mineralogical composition shows 14.71 % of Al<sub>2</sub>O<sub>3</sub>, 6.580 of K<sub>2</sub>O, and 1.366 of CaO, thus describing it as containing small traces of Potassium in the combination of Sodium, Silicon, and Aluminium and a specified specific gravity of less than 3.

Various authors [17] in Jordan [20] have undertaken the mineralogical investigation of TA from the various parts of Jordan, as shown in Table 3 and determined that the mineralogical composition varies even within the same geographical area. It is noted that it is necessary to undertake mineralogical composition for the TA aggregates before incorporating in concrete.

Volcanic tuff is a natural pozzolanic material with cementitious elements such as Silicon Oxide and Calcium Oxide. Silicon Oxide is responsible for early compressive strength, and Calcium Oxide for long-term strength development and reducing alkali-silica reactions. Compared to that of Normal Portland Cement (NPC), the chemical compositions for the TA are similar with small variations. However, [20] note that using TA aggregate as a % replacement of cement may not be viable as a natural pozzolanic material as the % sum of SiO<sub>2</sub>, Al<sub>2</sub>O<sub>3</sub>, and Fe<sub>2</sub>O<sub>3</sub> is 91.102 against 71 % recommended in the ASTM C-618.

### 3.2 CUBE COMPRESSIVE STRENGTH

The values for C25, C30, C35, C40, and C45 classes of concrete compressive strength are presented.

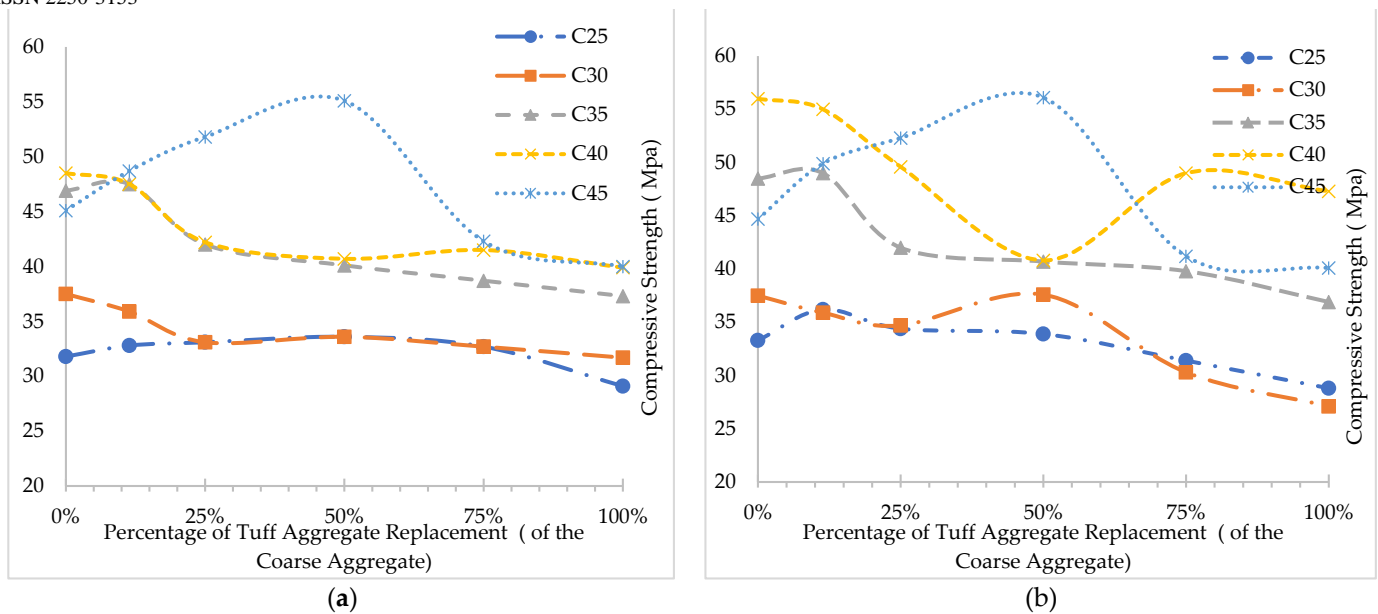


Figure 7 (a) A graph of Compressive Strength (28 days) against the % replacement of Tuff Aggregates; (b). A graph of Compressive Strength (56 days) against the % replacement of Tuff Aggregates.

Cubes for measuring modulus of elastic were observed to have the same trend of decreasing compressive strength as the % replacement increased. From the results shown in Figure 7(a) and (b), there is a steady decrease in the cube compressive strength with an increase in the replacement of lightweight aggregates even when a control load is applied.

The cube's failure begins by first cracking. These cracks are initiated and coincide with the weak points of the cellular tuff aggregate structures. As the load increases, the tensile strain concentration is initiated. The cracking process in the concrete containing tuff aggregate was observed to be slower and less explosive though the extent of this compared to normal-weight concrete was not quantified. Perhaps this was due to the more elastic nature of concrete containing tuff aggregates than conventional concrete with normal aggregates.

Ultimately the cube containing tuff aggregates failed at lower compressive stresses than those with NWC. This is attributed to the tuff aggregate's interconnected voids/pores producing weak points.

### 3.2 MODULUS OF ELASTICITY

From the results shown in Figure 7(a) and (b) it was observed that there is a steady decrease in the cube compressive strength with an increase in the replacement of lightweight aggregates. Therefore, it was expected that lower values of modulus of elasticity for an increase in the percentage replacement of TA with CA. NWC produced stiffer aggregates than LWC.

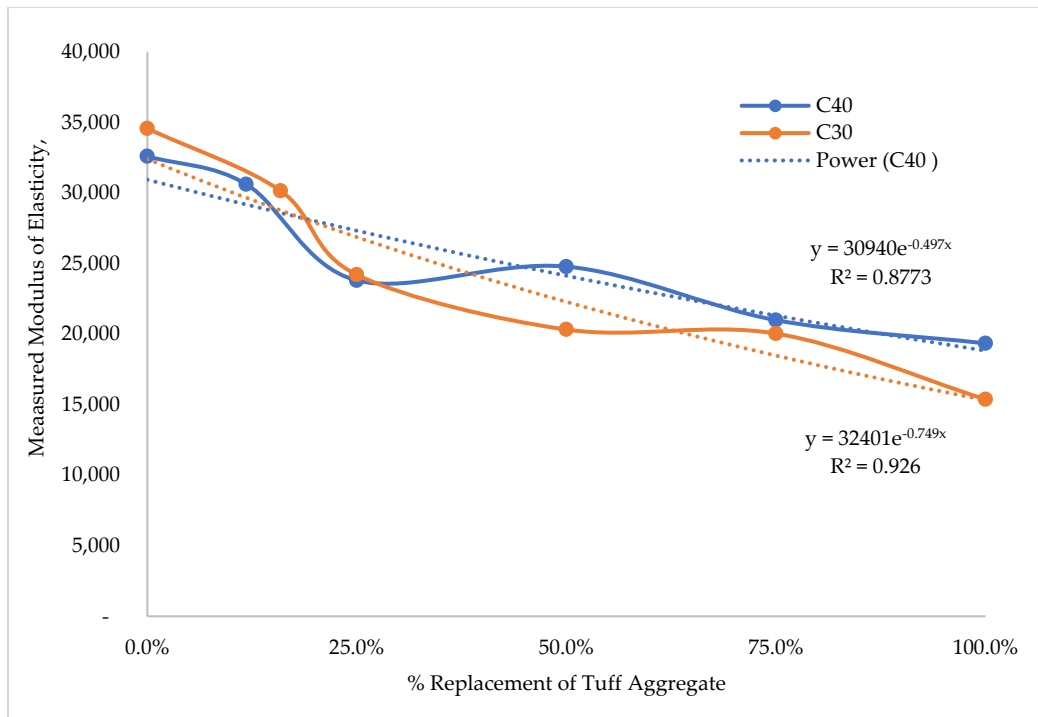


Figure 8. A graph of percentage replacement of Tuff Aggregates against the Measured Modulus of Elasticity for Class 30 and 40 of concrete.

The Figure 8, gives the relationship between the percentage replacement of CA and modulus of elasticity. Power relationships between the Measured Modulus of Elasticity and percentage replacement of TA is developed as described in Equation 1.

$$\text{Average of the Coefficients} = 31670.5$$

$$\text{Average of the Power Coefficients} = -0.623$$

$$\text{New Developed Relationship} \quad (1)$$

$$y = 31670.5 \times e^{-0.623x}$$

Where;

$y$  Is the Modulus of Elasticity  
 $x$  Is the percentage of replacement of CA with TA

In Figure 8, the variations of both NWC and LWC for the same percentage replacement of CA with TA in a given class of concrete were high. This observation is consistent with the findings of Muller-Rochholz [22], who measured the elastic modulus of LWA and NWA using ultrasonic pulse velocity. In Muller et al. study, elements of known modulus of elasticity were used to correlate the results and determined an accuracy of 1%. Further, the modulus of elasticity of the cement paste was lower than that of lightweight aggregate with the same cement content. The variability of stress homogeneity accounts for huge variations in the measurement of the modulus of elasticity of the specimens under this study. This is observed in Figure 8.

Holm et al. [23] noted that the presence of air entrained in the concrete is also responsible for variations in the modulus of elasticity in the concrete specimens. The presence of air in the cement matrix of NWC results in a non-homogenous material with varied stress concentrations, thus leading to micro-cracking. In contrast to LWC, the air in the cement matrix matches the stiffness of LWA, thus reducing micro-cracking.

### 3.3 SHRINKAGE

The shrinkage strain values for unsealed C45 beam specimens loaded for 60 days after 56 days of water ponding curing are shown in the Figure 9.

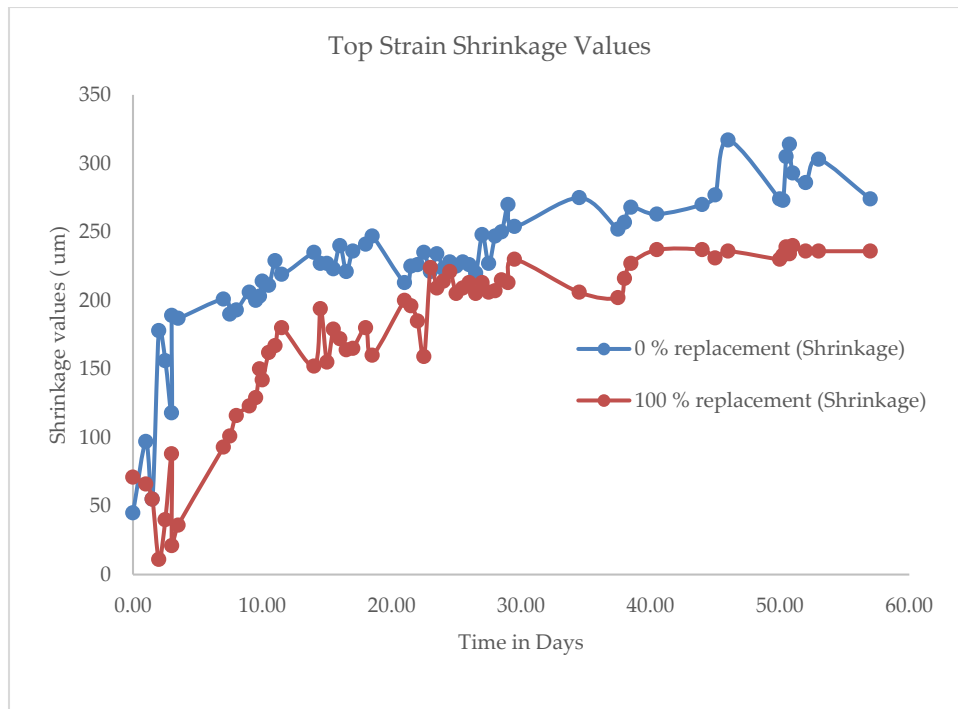


Figure 9. 60- Day Shrinkage Strain Values for the 0 % and 100 % replacement of Conventional aggregate with Tuff Aggregate. The maximum values of 0.000317 mm/m and 0.000236 mm/m for the 0 % and 100 % replacement were measured using shrinkage strain gauges.

For 100 % replacement of coarse aggregate, more water for internal curing was produced when the beams were exposed to a drying environment. The internal curing reduced the autogenous shrinkage, contributing to lower values of shrinkage strain for lightweight concrete. Autogenous shrinkage was estimated to be 40 micro-strains [17]; under this study, the difference between the two specimens was fairly constant.

The measured shrinkage values were due to drying shrinkage due to water loss in the gel pores. When the beam specimens are exposed to atmospheric conditions, a continuous process of losing gel water is ensured, and thus, cement pastes shrink in volume. Shrinking in volume contributes to microcracks that introduce points of weakness, and thus concrete creeps more.

Shrinkage in concrete cannot be eliminated; however, its magnitude can be reduced by using tuff aggregate, which produces water reserves for internal curing and reduces the heat of hydration. It reduces the heat of hydration by reacting with its aluminous and siliceous material (see the chemical composition of tuff in Table 3) in the presence of moisture at normal temperatures [6];[11].

ACI 209-92 Shrinkage model evaluated the value of total shrinkage at 0.000394 mm against a measured value of 0.000317 mm (difference of 77 micro-strains representing a 19.5 % difference) for the NWC. BS EN creep model evaluated the value of total shrinkage at 0.000400 mm against the experimental value of 0.000317 mm (difference of 83 micro-strains representing a difference of 20.8 % difference) for the NWC.

### 3.3.1 Effect of Relative Humidity (RH) and Temperature on Shrinkage

In this study, the RH values under which the beam specimens for shrinkage and creep were undertaken were estimated to be 50 %- 70 %, while the temperature was 15o C to 28oC from March through April 2022. The range of temperatures and RH could partly be responsible for the daily spikes in shrinkage strain readings determined by the data logger and shown in Figure 11. Also, the strain gauge slip was noted to be responsible for the daily spikes.

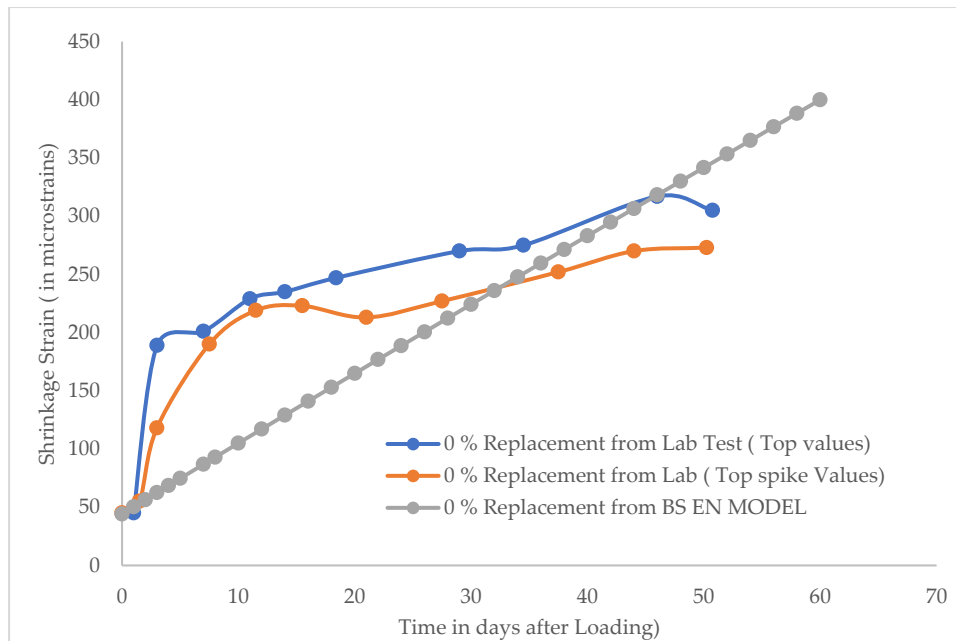


Figure 11. Comparison of the Upper and Lower Spike values with the predicted values of Shrinkage Strain from the BS EN Creep Model.

### 3.1.2 Effect of Water-Cement Ratio on Shrinkage

The study investigated classes C25, C30, C35, C40, and C45 for compressive strength, measured after 28 and 56 days. Only C45 Concrete mix cast and cured for 56 days was used for a further 60-day shrinkage strain measurements using strain gauges attached on 2 No beams- one control and the other one with full replacement of CA with TA, and the values output to a Data Logger. The C45 Mix was air dried at 15-28 degrees at an approximate relative humidity of 70 %. The computed w/c ratio for C45 was 0.38.

The correlation of w/c ratio- compressive strength was studied by [24], and the coefficient of determination (R<sup>2</sup>) was found to be in the range of 0.9931-0.9998 for the HPC in the study. This observation aids in inferring that the shrinkage strain in this study was expected to follow the same trend whereby the w/c is inversely proportional to the compressive strength for all classes of Concrete.

Researchers have undertaken shrinkage strain measurements on the concrete of various w/c ratios. Piasta & Zarzycki [24] measured shrinkage strain (micro-strains) for w/c of 0.25, 0.30, and 0.35 ratios for 120 days after casting without curing. For each increase in the w/c ratio, there was an increase in the maximum shrinkage strain attained. The maximum shrinkage strains are 410 um, 495 um, and 520 um, respectively, for the w/c mentioned above. Ayarkwa [25] studied shrinkage strain to ASTM C517-04 for 75 x 75 x 285 mm prismatic beam specimens cured up to 28 days after casting. Concrete mixes with w/c ratios of 0.56 and 0.52 yielded 368 um and 325 um, respectively. The author compared the measured values to those predicted by various models through the residual of squares. In the same study, CEB-FIP 90, GL 2000 and B3 models over-predicted the values whereas the BS EN and ACI models under-predicted.

### 4.1 CREEP

The shear strain was observed along 450 at the centre of the support for 60 days after 56 days of moist curing. There was a fairly linear increase for the 45 days, as shown in Figure 4.5. NWC produced lower values than LWC.

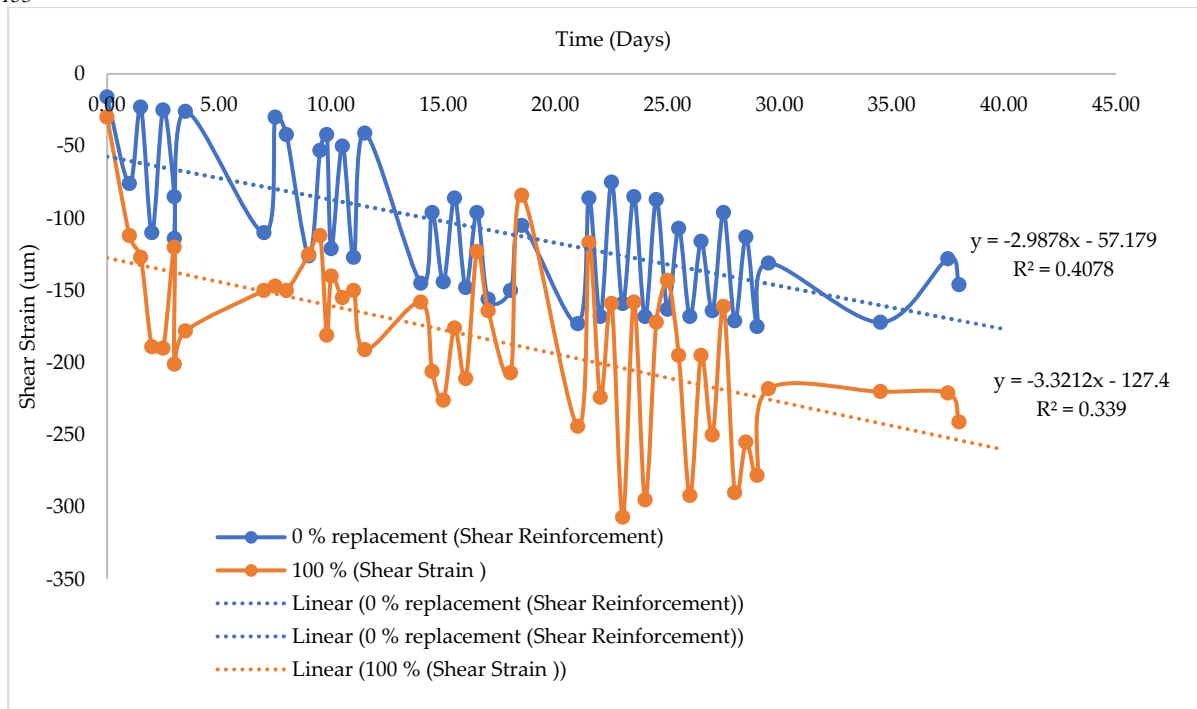


Figure 12. Shear Deformation at the supports of the creep beam specimen.

Strain in the reinforcements for NWC and LWC maximum values of 0.000473 mm/m and 0.000427 mm/m were observed. At the same time, the fitted line curves produced an average value of 0.000400 mm/m and 0.000300 mm/m, respectively, at 60 % of the moment capacity of the beam specimen. ACI provides a value of 0.0003mm/m, while Eurocode provides 0.0002-0.0003 for NWC and 0.00035 for LWC.

The rate of increase of reinforcement strain for LWC for the first 10 days is higher than NWC. This confirms that NWC is more brittle than lightweight concrete, thus developing fewer cracks.

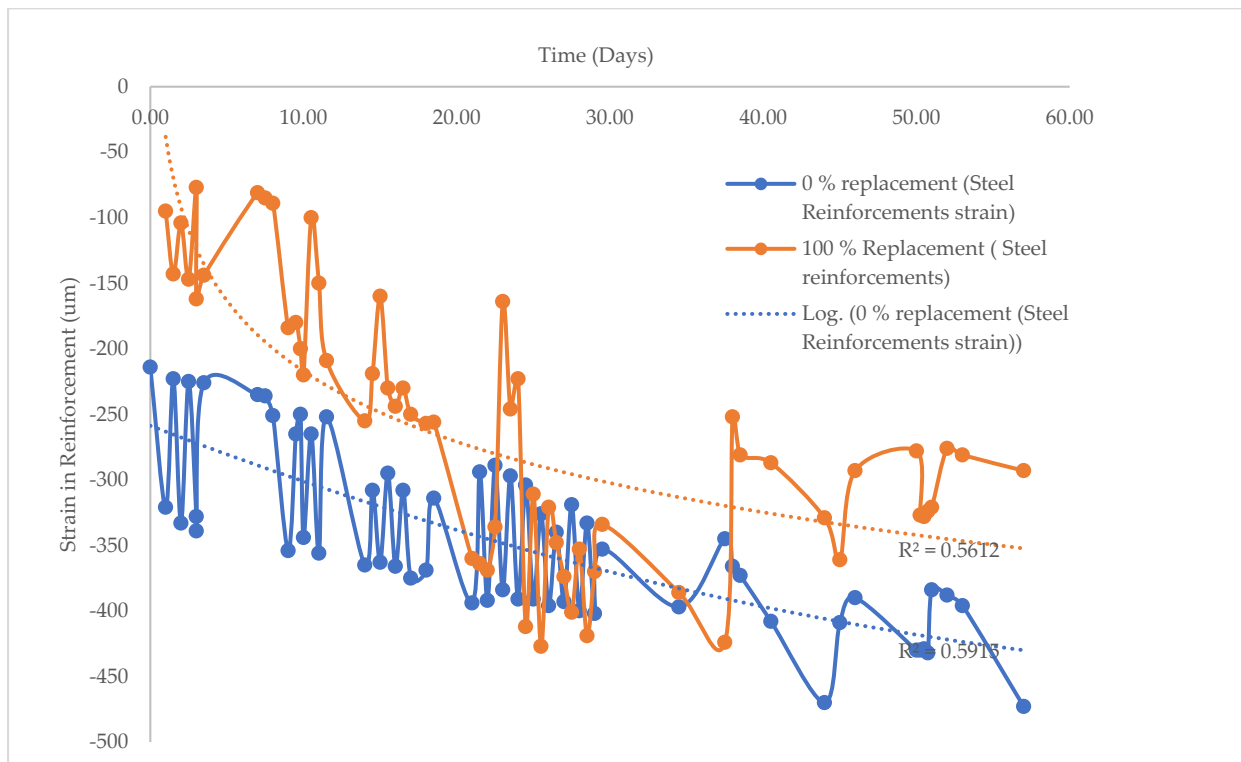


Figure 13. Strain in Reinforcement for the Beam Specimen Loaded for 60 days.

#### 4.1.1 Effect of Water-Cement Ratio of Concrete of Creep

Brooks [11] noted that creep increased as the concrete classes reduced for a constant cement paste or aggregate volume. Low concrete classes have high porosity due to some void that hydration products cannot fill. Composite models have been used to evaluate the factors affecting the modulus of elasticity.

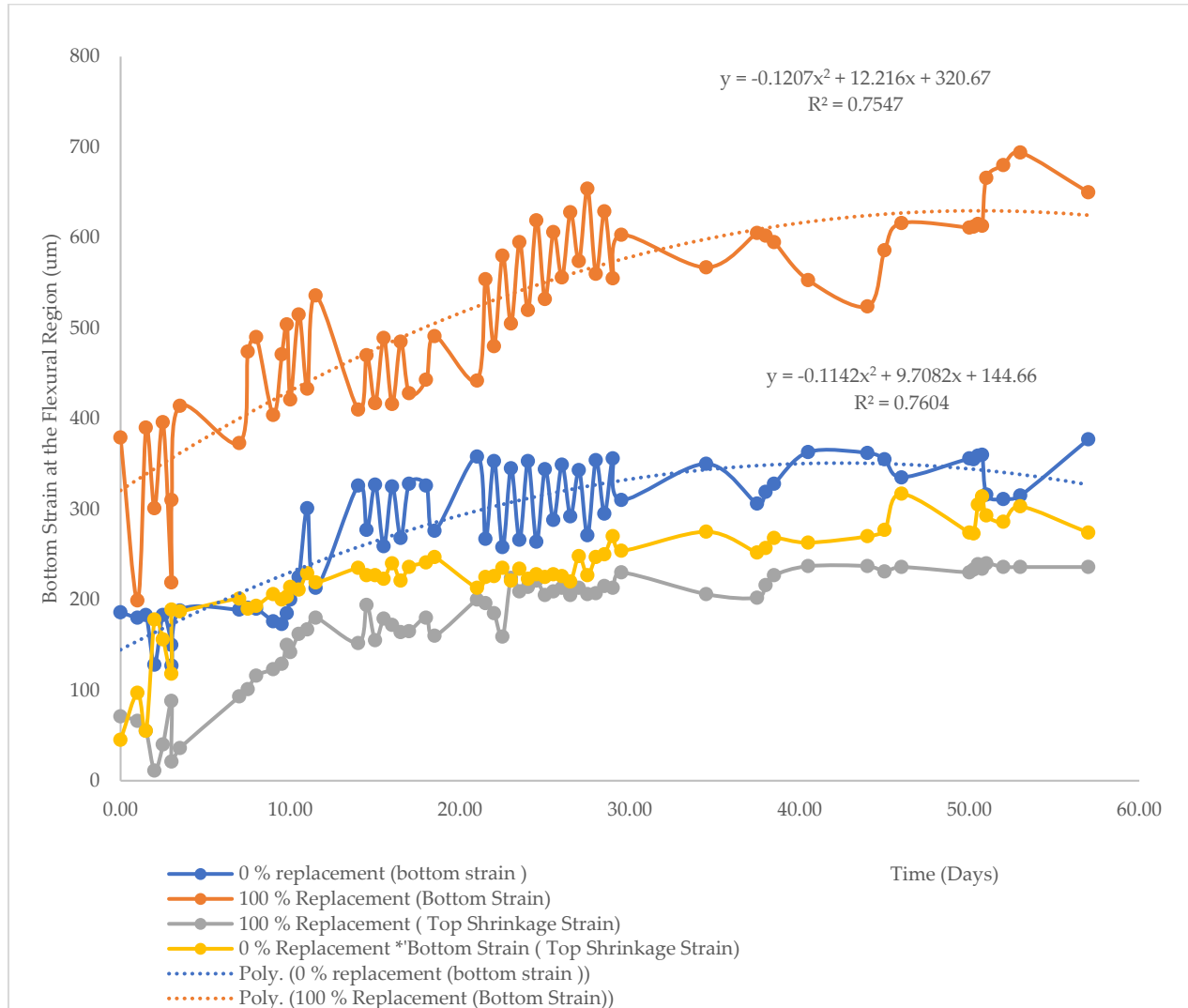


Figure 14. Total Bottom Strain in the Beam Specimen for Class 45 loaded for 60 days.

The bottom surfaces of the beam were attached with strain gauges to measure strain due to flexural creeping. LWC had a higher strain than NWC measured maximum strain of 694 and 360 micro-strains, respectively as shown in Figure 14. For NWC, creep is caused by the hardened cement paste since the aggregate is stiffer than the cement paste. The aggregates contribute towards concrete creep for lower values of modulus of elasticity of tuff aggregate.

The high initial strains for LWC are attributed to water movement from tuff aggregate, which contributes to creeping. This is evident in the first 15 days after loading as shown in Figure 14.

The creep rate was faster for the first 30 days than the later ages (between 30 -60 days), where the creep rate tends to be constant. The creep strain for 30-60 days reached a secondary stage of a steady creep state. The creep values are less curvilinear since the beam specimen was loaded at 60 % of the flexural capacity of the beam.

ACI 209-92 Creep Model estimates the total strain of the (0.2 x 0.2 x 1 m) beam specimen to be 395 micro-strains. At the same time, the maximum experimental value is determined to be 360 micro-strains. This is a difference of 35 micro-strains, thus a difference of 9.7 %. BS EN creeps analytical model evaluated the beam specimen total strain as 395 micro-strains while the experimental value was 395 micro-strains. It is an exact match between the computed and measured values in the study.

This publication is licensed under Creative Commons Attribution CC BY.

The internal relative humidity of the concrete matrix mostly causes the creep of concrete for NWC. As a result of loading, the pore water moves from a region of high concentration to that of low concentration while also the loading intensity shifts from the liquid phase to the adjacent solid phase. For the case of sustained loading, the pressure of both gel pore water and capillary water disappears, and thus adsorbed water continues to cause creep during the period concrete is under loading. This may not be the case in LWC, as the less stiff aggregates contribute towards greater creep values than the water movement.

#### 4.1.2 CREEP COEFFICIENT

Creep can be defined by creep coefficient which a ratio of the creep strain to that of elastic strain. The beam specimen was loaded at 60 % of the beam’s flexural strength. The strains were non-linear due to very fine bond cracks forming at the interface of hardened cement paste and aggregates. The fine bond cracks caused differential volume changes between the cement paste and aggregate due to temperature and humidity variations.

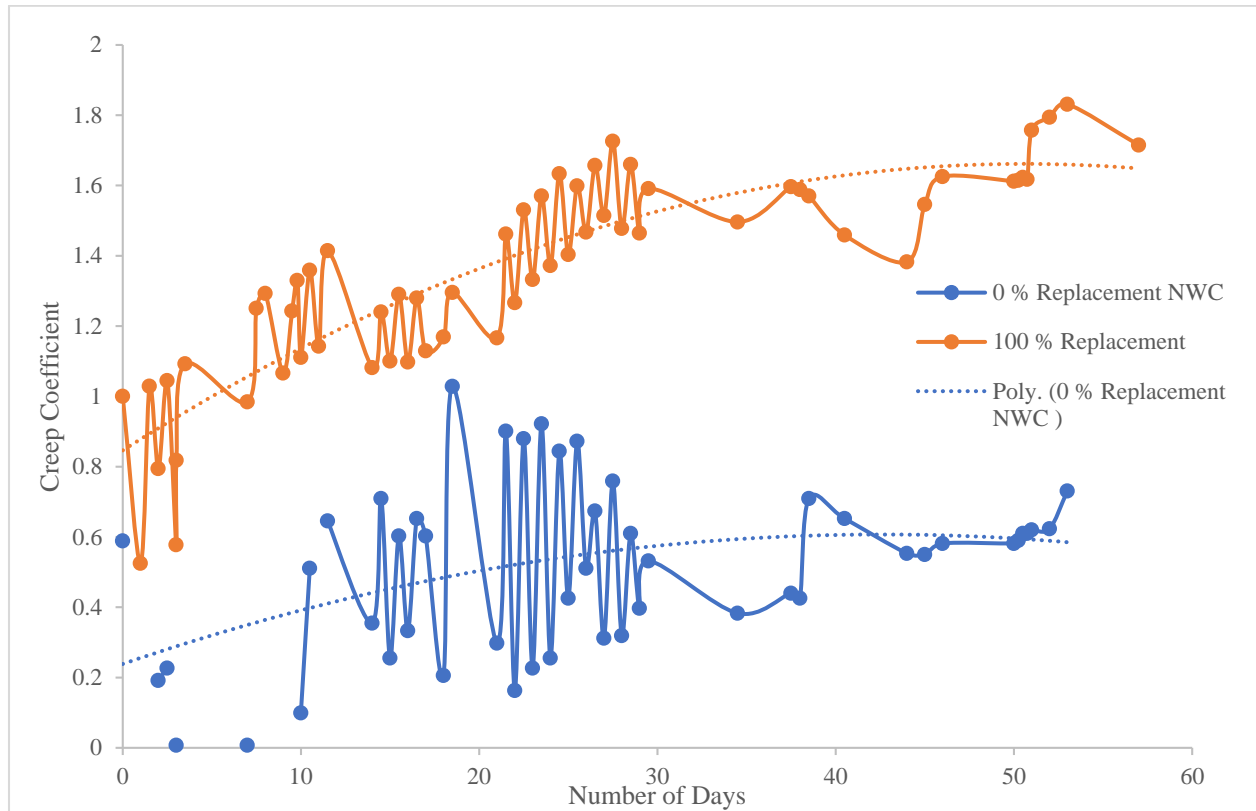


Figure 15. Creep Coefficient for the LWC and NWC beam Specimen loaded for 60 days for Class 40 Beam Specimen.

The NWC beam specimen attained a creep coefficient of 0.6, while the LWC beam specimen attained 1.63 as shown Figure 15. ACI Model under ACI 209-92 model evaluated the beam specimen to be at 0.64.

#### 4.1.3 SPECIFIC CREEP

Creep can be quantified through Specific creep which is the creep strain values divided by the applied stress. The applied stress is 10.7 Nmm<sup>2</sup>. The values of specific creep for the two-beam specimen can be evaluated from Figure 16. Figure 16 values are computed from Equation 2 and plot of Specific creep against time is presented in Figure 17. The creep strain is determined by;

$$\text{Creep Strain} = \text{Measured Total Bottom Strain} - \text{Measured Shrinkage Strain} \quad (2)$$

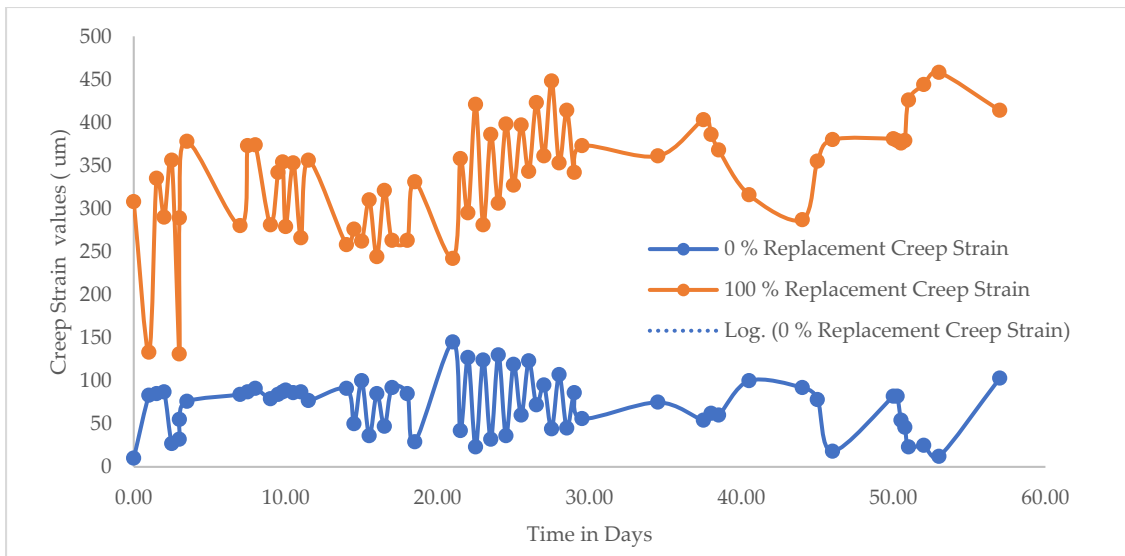


Figure 16. 60-Day Creep Strain values for the 0 % and 100 % replacement creep strain for class 40 Beam Specimen.

The Average value of Specific Creep for 100 % Replacement of NA is 1.6, while the maximum and minimum values are 2.22, while that with 0 % Replacement is 0.19, with the maximum attained value being 0.39. A summary of this results and those computed using the methods in BS EN and ACI models are presented in Table 4.

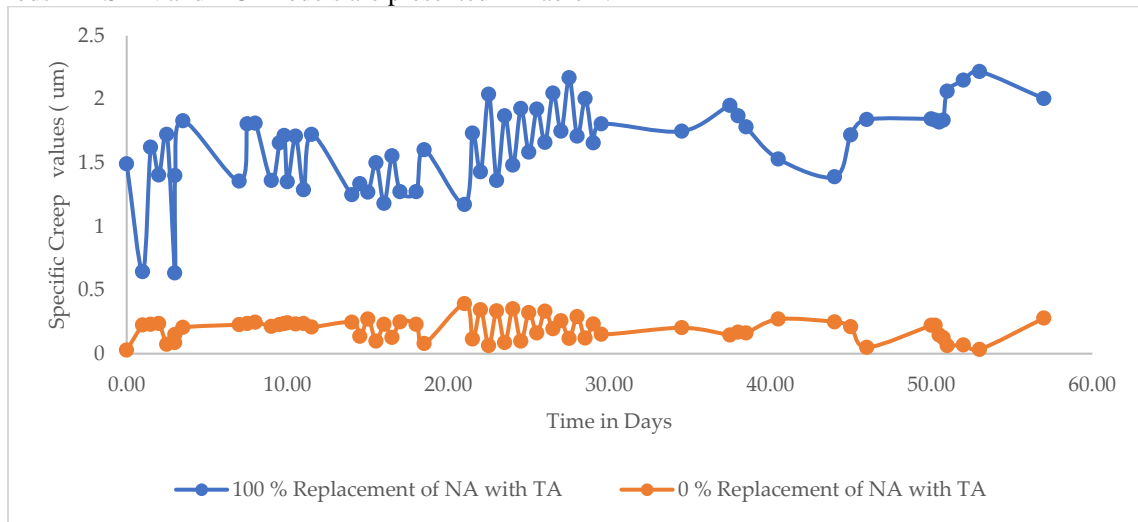


Figure 17. 60-Day specific creep values for the 0 % and 100 % replacement.

The measured values of specific creep have been evaluated and compared with those of Counto Specific Creep, BS EN, and ACI 209-92 Models. This observation is consistent with the results of 3.1 and 3.2 of the study. The Counto Model yields a value of 0.806 per Mpa for both NA and TA. BS EN Model yields 0.943 per Mpa, and the ACI 209-92 Model yields 0.51, as shown in Table 4.

Method of Evaluation/ Measurement of Specific Creep per Mpa	NWC	LWC	Remarks
From Laboratory Data/ Author’s Model	0.34	0.914	Av. Values used
From Counto Specific Creep Model	0.806	0.806	
BS EN Creep Model	0.943	0.869	
ACI 209-92 Model	0.51	0.87	

The Counto Specific Creep Models evaluated specific creep as 0.81 and 0.806 for NWC and LWC. In this model, the sensitivity to computations of fractional volume of aggregates  $g$  is less. ( $g$  is 0.619279 and 0.620632 for NWC and LWC respectively). When evaluating specific creep using Equations 1 and 2 of the study.

ACI 209-92 Model values are consistent with the findings of the author's study. The specific creep values for NWC are lesser than those of LWC. This model accounts for differences in density of LWA and NWA. BS EN Creep Model values are inconsistent with the author's findings. The specific creep values for NWC are more than those of LWC. The difference is associated due to computations of compliance with that method of ACI 209-92.

#### IV. CONCLUSION

The following conclusions were made;

- LWC containing tuff aggregate has lower compressive strength, modulus of elasticity, and creep values than NWC.
- LWC containing tuff aggregates lower shrinkage than NWC. Shrinkage in concrete cannot be eliminated; however, its magnitude can be reduced by using tuff aggregate, which produces water reserves for internal curing and reduces the heat of hydration.
- ACI 209-92 Model for computation of specific creep is consistent with the author's results.

#### REFERENCES

- [1] N. Asniar, Y. M. Purwana, and N. S. Surjandari, "Tuff as rock and soil: Review of the literature on tuff geotechnical, chemical and mineralogical properties around the world and in Indonesia," *AIP Conf Proc*, vol. 2114, no. June, pp. 1–10, 2019, doi: 10.1063/1.5112466.
- [2] Ş. Kilinçarslan, "The effect of zeolite amount on the physical and mechanical properties of concrete," *International Journal of Physical Sciences*, vol. 6, no. 13, pp. 3041–3046, 2011, doi: 10.5897/IJPS10.164.
- [3] J. Al-Zou'By and K. K. Al-Zboon, "Effect of volcanic tuff on the characteristics of cement mortar," *Ceramica*, vol. 60, no. 354, pp. 279–284, 2014, doi: 10.1590/S0366-69132014000200018.
- [4] C. Karakurt and U. Özen, "Influence of Natural Lightweight Aggregates on the Properties of Concrete," *Journal of the Turkish Chemical Society*, vol. 1, no. 2, pp. 51–58, 2017.
- [5] R. A. Al Dwairi, B. Al Saqarat, F. Shaqour, and M. Sarireh, "Characterization of Jordanian Volcanic Tuff and its Potential Use as Lightweight Aggregate," vol. 9, no. 2, pp. 127–133, 2018.
- [6] S. G. K, A. S. O, and M. J. N, "Investigating the Potential Use of Tuff Aggregates to Produce Lightweight Concrete," *International Journal of Scientific and Research Publications (IJSRP)*, vol. 10, no. 9, pp. 458–478, 2020, doi: 10.29322/ij srp.10.09.2020.p10555.
- [7] H. Yang, X. Xu, H. Cui, Z. Lin, and T. Y. Lo, "Effect of cured time on creep of lightweight aggregate concrete," *International Conference on Durability of Concrete Structures, ICDCS 2016*, pp. 134–140, 2016, doi: 10.5703/1288284316122.
- [8] R. Gilbert and G. Ranzi, "Time-Dependent Behavior of Concrete Structures. 2010." doi: 10.1201/9781482288711.
- [9] D. Li, S. Kaewunruen, P. Robery, and A. M. Remennikov, "Parametric Studies into Creep and Shrinkage Characteristics in Railway Prestressed Concrete Sleepers," *Front Built Environ*, vol. 6, no. August, pp. 1–10, 2020, doi: 10.3389/fbuil.2020.00130.
- [10] T. Mohammed, "The Determination of The Concrete Tensile Creep at Early Age Using the Ring Test," pp. 1–141, 2018.
- [11] J. J. Brooks, *Methods of Predicting Elasticity, Shrinkage, and Creep of Concrete*. 2015. doi: 10.1016/b978-0-12-801525-4.00011-x.
- [12] G. C. Fanourakis, "The Influence of Aggregate Stiffness on the Measured and Predicted Creep Behaviour of concrete," *University of Witwatersrand*, 1998. doi: .1037//0033-2909.I26.1.78.
- [13] M. F. Granata and A. Recupero, "Serviceability and Ultimate Safety Checks of Segmental Concrete Bridges through N-M and M-V Interaction Domains," *Journal of Bridge Engineering*, vol. 20, no. 8, pp. 1–11, 2015, doi: 10.1061/(asce)be.1943-5592.0000686.
- [14] H. Huang, R. Garcia, S. S. Huang, M. Guadagnini, and K. Pilakoutas, "A practical creep model for concrete elements under eccentric compression," *Materials and Structures/Materiaux et Constructions*, vol. 52, no. 6, pp. 1–18, 2019, doi: 10.1617/s11527-019-1432-z.
- [15] B. E. Usibe, J. O. Ushie, and I. P. Etim, "Prediction of Creep Deformation in Concrete Using Some Design Code Models," *IOSR Journal of Mechanical and Civil Engineering*, vol. 6, no. 3, pp. 375–379, 2012, doi: 10.9790/1684-0434953.
- [16] K. K. Adewole, W. O. Ajagbe, and I. A. Arasi, "Determination of appropriate mix ratios for concrete grades using Nigerian Portland-limestone grades 32.5 and 42.5," *Leonardo Electronic Journal of Practices and Technologies*, vol. 14, no. 26, pp. 79–88, 2015.
- [17] A. Ababneh and F. Matakah, "Potential use of Jordanian volcanic tuffs as supplementary cementitious materials," *Case Studies in Construction Materials*, vol. 8, no. December, pp. 193–202, 2018, doi: 10.1016/j.cscm.2018.02.004.
- [18] W. F. Edris, S. Abdelkader, A. H. E. Salama, and A. A. K. A. Al Sayed, "Concrete behaviour with volcanic tuff inclusion," *Civil Engineering and Architecture*, vol. 9, no. 5, pp. 1434–1441, 2021, doi: 10.13189/CEA.2021.090516.
- [19] O. Maaitah, N. A. Hadi, and M. Abdelhadi, "Utilization of natural and industrial mineral admixtures as cement substitutes for concrete production in Jordan," no. April, 2015, doi: 10.5897/JCECT2014.0344.
- [20] W. F. Edris, S. Abdelkader, A. H. E. Salama, and A. A. K. A. Al Sayed, "Concrete behaviour with volcanic tuff inclusion," *Civil Engineering and Architecture*, vol. 9, no. 5, pp. 1434–1441, 2021, doi: 10.13189/CEA.2021.090516.
- [21] D. Saradhi Babu, "Mechanical and Deformational Properties, And Shrinkage Cracking Behaviour of Light-weight Concretes," *National University of Singapore*, vol. 49, no. 49, pp. 69–73, 2008.

- [22] J. Müller-Rochholz, "Determination of the elastic properties of lightweight aggregate by ultrasonic pulse velocity measurement," *International Journal of Cement Composites and Lightweight Concrete*, vol. 1, no. 2, pp. 87–90, 1979, doi: 10.1016/0262-5075(79)90014-9.
- [23] T. A. Holm, O.-S. Ooi, and T. Bremner, "Moisture dynamics in lightweight aggregate and concrete," *Expanded Shale Clay & Slate Institute*, no. February, p. 12, 2004.
- [24] W. Piasta and B. Zarzycki, "The effect of cement paste volume and w/c ratio on shrinkage strain, water absorption and compressive strength of high-performance concrete," *Construction Building Materials*, vol. 140, pp. 395–402, 2017, doi: 10.1016/j.conbuildmat.2017.02.033.
- [25] J. Ayarkwa, "Accuracy of creep predicting models in Ghana Accuracy of Creep Predicting Models in Ghana," no. March 2018, 2015.
- [26] U. J. Counto and M. A. Chiorino, "The effect of the elastic modulus of the aggregate on the elastic modulus, creep and creep recovery of concrete," *Magazine of Concrete Research*, vol. 17, no. 52, pp. 142–151, 1965, doi: 10.1680/mac.1965.17.52.142.
- [27] F. H. Wittmann and T.-J. Zhao, "Knowledge of Microstructure of Concrete for the Design of Durable Reinforced Concrete Structures," *Second International Conference on Microstructural -related Durability of Cementitious Composites*, no. April 2012, 2012.
- [28] M. Guadagnuolo, M. Aurilio, A. Basile, and G. Faella, "Modulus of elasticity and compressive strength of tuff masonry: Results of a wide set of flat-jack tests," *Buildings*, vol. 10, no. 5, 2020, doi: 10.3390/BUILDINGS10050084.